Extended frequency analysis of the loss under rotating induction excitation in Soft Magnetic Composites (SMC)

Olivier de La Barrière, Carlo Appino, F . Fiorillo, Carlo Ragusa, Michel Lécrivain, L. Rocchino, Hamid Ben Ahmed, M. Gabsi, Frédéric Mazaleyrat, Martino Lobue

Extended frequency analysis of the loss under rotating induction excitation in Soft Magnetic Composites (SMC)

O. de la Barrière[1a], C. Appino[1], F. Fiorillo[1], C. Ragusa[2], M. Lecrivain[3], L. Rocchino[1], H. Ben Ahmed[3], M. Gabsi[3], F. Mazaleyrat[3] and M. LoBue[3]

[1]Istituto Nazionale di Ricerca Metrologica (INRIM), Torino, Italy
[2]Dipartimento di Ingegneria Elettrica, Politecnico di Torino, C.so Duca degli Abruzzi 24, 10129 Torino, Italy
[3]SATIE, ENS Cachan, CNRS, UniverSud, 61 av du President Wilson, F-94230 Cachan, France

[a] Corresponding author: barriere@satie.ens-cachan.fr

Abstract

This article reports new results about the magnetic loss in Soft Magnetic Composites excited with rotating field. Indeed, these materials are very promising in electrical engineering applications, such as new topologies of electrical machines in which multidimensional induction loci are ubiquitous. Therefore, it has been provided an experimental characterization of a commercial SMC sample devoted to electrical machine applications, up to the kilohertz range, under alternating and circular induction loci. To this end, an experimental system has been designed and optimized for this kind of loss measurements, and the results have been subjected to the loss separation procedure, focusing the attention on the ratio between circular and alternating loss. The ratio between the excess loss obtained under rotating and alternating inductions of same peak amplitude has been found almost frequency independent. This result is then applied to successfully predict the loss under more complex induction loci, such as the elliptical case.

I. Introduction

Machine designers are nowadays working on new machine topologies, such as hybrid excitation [1] motors. Since 3D flux paths are encountered in such machines, an isotropic soft magnetic material is needed. Contrary to laminated materials, Soft Magnetic Composites can fulfill these isotropy requirements [2]. These materials are also interesting for their low classical loss component, due to their granular structure, making them suitable for high speed electrical machines [3].

Therefore, the analysis of the loss under 2D and 3D flux loci in SMC has become a challenging topic [4][5], with the consequent problem of the choice of an appropriate measurement setup. Most authors [4] use a square sample set up in the center of a cross-shaped apparatus made of soft magnetic material, but the magnetic induction in this system is not perfectly homogeneous [6]. To improve the induction homogeneity, other authors [7] have developed equipments made of a circular sample put in the center of a three phase motor stator. In each case, the maximum frequency does not exceed 200 Hz, which is sufficient for laminations [8], but not for SMC.

Although the loss separation principle remains applicable, another problem arising for the 2D loss analysis is the extension of the Statistical Theory of Losses (STL) [9] to circular induction excitations. In fact, the STL gives a rationale for the magnetization processes along one dimension only, and cannot be directly applied to 2D magnetization paths. Therefore, in this case, empirical approaches have to be proposed. For example, in the case of laminations, the non-monotonous behavior of the hysteresis part versus the peak induction under circular excitation conditions has been experimentally put in evidence [4][8], and it has also been shown that the ratio between excess losses under circular and alternating inductions is independent of the frequency.

This paper is centered on the following points:

- Experimental loss characterization up to 4 kHz under circular induction excitation of a commercial SMC, using a optimally designed apparatus.

– Analysis of results by adopting the SLT and the ensuing loss separation procedure, with consequent identification of the loss components vs. the peak induction (B_P) and the magnetizing frequency (f). Like in the case of laminations [8], an excess loss ratio between rotating and alternating inductions quite independent of the frequency has been found.

– Eventually, the above presented procedure has been experimentally validated by predicting the loss under elliptical induction loci.

II. EXPERIMENTAL WORK

In order to obtain the best homogeneity of the sample induction, the method of the three phase magnetizer [7] has been retained. Disk shaped samples have been cut from a SMC cylinder produced by the Höganäs company [10]. Double axis B-coils and H-coils [7] have been used for the induction and magnetic field acquisition, and the loss is then found by applying the fieldmetric method [11].

An optimization procedure, based on the finite element method, has been developed, in order to find the topology and dimensions of the three phase excitation system shown in Fig. 1.

The measurements, under alternating and rotating inductions, have been conducted up to f=4 kHz, and for five B_P levels: 0.25 T, 0.5 T, 0.75 T, 1 T, and 1.25 T. The alternating loss is computed by averaging the figures obtained along two perpendicular directions. For the circular case, the loss is computed by averaging the results found upon clockwise and counterclockwise rotation of the magnetic induction (Fig. 2).

III. LOSS SEPARATION

A. Loss separation under alternating sinusoidal induction

The loss results under alternating sinusoidal induction excitation has been analyzed following the same procedure outlined in [12]. Accordingly, the classical loss component $W_{class}^{(alt)}(B_P,f)$ is computed under the assumption that eddy currents are confined in the grains, whose size and shape distributions

have been found out thanks to micrographs analysis. The value of the hysteresis loss $W_{hyst}^{(alt)}(B_P)$ is obtained by extrapolating to zero frequency the quantity:

$$W_{diff}^{(alt)} = W^{(alt)} - W_{class}^{(alt)} = W_{hyst}^{(alt)} + W_{exc}^{(alt)}, \qquad [J/m^3] \qquad (1)$$

where $W^{(alt)}=W^{(alt)}(B_P,f)$ is the experimental total loss and $W_{exc}^{(alt)}=W_{exc}^{(alt)}(B_P,f)$ the excess component. Remembering that B_P is equal to the peak polarization, the STL gives an expression for $W_{exc}^{(alt)}$ (2), which is exploited to fit $W_{diff}^{(alt)}$:

$$W_{exc}^{(alt)}(B_P, f) = 2n_o V_o \left(\sqrt{1 + \frac{16\sigma_{Fe} GSV_o}{(n_o V_o)^2} B_P f} - 1 \right) \qquad [J/m^3] \qquad (2)$$

In (2), σ_{Fe} is the iron conductivity, G=0.1356, S is the sample cross section, and the couple of parameters n_o and V_o are connected with the material microstructure. The fitting procedure leads to the behavior of the parameters n_o and V_o vs. B_P. It must be noticed the square root behavior of $W_{exc}^{(alt)}$ vs. f, like for laminations [9].

B. Loss separation under rotating induction

The same loss separation procedure has been followed in the circular induction case. The two perpendicular induction components of the circular locus are also in quadrature in the time domain. Therefore, thanks to the Parseval theorem, one gets, for the classical loss component $W_{class}^{(circ)}(B_P,f)=2\cdot W_{class}^{(alt)}(B_P,f)$. The excess loss under rotating induction can be defined similarly to the alternating induction case:

$$W_{exc}^{(circ)}(B_P, f) = W_{tot}^{(circ)}(B_P, f) - \left(W_{hyst}^{(circ)}(B_P) + W_{class}^{(circ)}(B_P, f) \right) \qquad (3)$$

The application of formula (2) is not possible, because the magnetization processes under rotating induction are totally different from the ones encountered under alternating induction, and the application of the SLT has no clear physical meaning at present. However, the hysteresis loss component under circular excitation $W_{hyst}^{(circ)}(B_P)$ is again given by the extrapolation of the total loss $W^{(circ)}(B_P,f)$ to zero frequency.

In order to investigate the loss behavior under different magnetization regimes, we introduce the ratios $R_{hyst}(B_P)=W_{hyst}^{(circ)}(B_P)/W_{hyst}^{(alt)}(B_P)$, $R_{class}(B_P,f)=W_{class}^{(circ)}(B_P,f)/W_{class}^{(alt)}(B_P,f)=2$, and $R_{exc}(B_P,f)=W_{exc}^{(circ)}(B_P,f)/W_{exc}^{(alt)}(B_P,f)$.

These quantities can be exploited to predict the loss figures under elliptical regime starting from a limited number of measurements.

Parameters R_{hyst} and R_{exc} are depicted in Fig. 3 and Fig. 4 vs. peak induction B_P. In Fig. 4, the frequency, is ranging from 20 Hz (which can be considered as nearly static) to 4 kHz. The ratios are both seen to decrease vs. B_P, as observed in [8], especially for the highest peak inductions, due to the higher part of coherent rotations involved in the circular magnetization process. It must be noticed, however, that the highest peak induction considered here (B_P=1.25 T) is not sufficient to see this ratio decreasing below the unity, as seen in [8] for the highest induction values in laminations. In particular, considering R_{exc}, the most striking fact is that this ratio is almost independent of the frequency, like it is the case of laminations [8]. This remark has important consequences for the prediction of the loss under more complicated induction loci, as illustrated below when dealing with the elliptical induction case.

IV. PREDICTION OF THE LOSS UNDER ELLIPTICAL INDUCTION LOCI

We have applied an elliptical induction locus with major and minor axes B_P and B_m, respectively. The prediction is carried out by computing separately each term of the loss, and by summing up these terms. The classical loss is given by the following formula [8], after introducing the quantity $a=B_m/B_P<1$:

$$W_{class}^{(ellip)}(a,B_P,f)=W_{class}^{(alt)}(B_P,f)\cdot\left(1+a^2\right) \tag{4}$$

In [13], the following interpolation formulae have been proposed (and applied to laminations) for the loss under elliptical induction given the loss data under alternating and circular cases:

$$\begin{cases} W_{hyst}^{(ellip)}(a,B_P)=W_{hyst}^{(alt)}(B_P)+\left[R_{hyst}(B_P)-1\right]W_{hyst}^{(alt)}(B_m) \\ W_{exc}^{(ellip)}(a,B_P,f)=W_{exc}^{(alt)}(B_P,f)+\left[R_{exc}(B_P)-1\right]W_{exc}^{(alt)}(B_m,f) \end{cases} \tag{5}$$

All the right terms of (5) can be computed using the loss separation under alternating and circular inductions carried out in the previous section (remark that the ratios are frequency independent).

Measurements under elliptical excitation conditions have been made for two frequencies (f=100 Hz and f=1 kHz), with B_P=1 T. In each case, the minor axis induction amplitude B_m varies from 0 (alternating case) to B_P (circular case). This is equivalent to a variation of a in the interval $0 \leq a \leq 1$. The results are displayed in Fig. 5, and a good agreement between predicted and experimental results is found.

V. CONCLUSION AND PERSPECTIVES

In this paper, measurements under alternating and circular inductions in SMC have been proposed, up to 4 kHz. This characterization was possible thanks to a specially optimized characterization setup. The loss separation procedure, both under alternating and rotating conditions, has been carried out. The main result is that in these materials, the ratio between excess loss under circular and alternating inductions is independent of f in a wide frequency range. This allows a significant simplification for the loss prediction model under more complex induction loci.

Further work is needed to develop an equipment able to perform measurements exploiting the so-called thermometric method technique [8], in order to overcome the measurement problems encountered with the fieldmetric method at high inductions. This would allow to study more accurately the decrease of the hysteresis and excess losses when the SMC material approaches the saturated state.

References

[1] Y. Amara et al., "Hybrid excitation synchronous machines: Energy-efficient solution for vehicles propulsion," *IEEE Transactions on Vehicular Technology*, vol. 58, no. 5, pp. 2137-2149, 2009.

[2] Y. Guo et al., "Influence of inductance variation on performance of a permanent magnet claw pole soft magnetic composite motor," *Journal of Applied Physics*, vol. 103, no. 7, p. 07F118, 2008.

[3] A. Chebak, P. Viarouge, and J. Cros, "Analytical Computation of the Full Load Magnetic Losses in the Soft Magnetic Composite Stator of High-Speed Slotless Permanent Magnet Machines," *IEEE Transactions on Magnetics*, vol. 45, no. 3, pp. 952-955, 2009.

[4] Y.G. Guo, J.G. Zhu, and J.J. Zhong, "Measurement and modelling of magnetic properties of soft magnetic composite material under 2D vector magnetisations," *Journal of magnetism and magnetic materials*, vol. 302, no. 1, pp. 14-19, 2006.

[5] Y.G. Guo, J.G. Zhu, Z.W. Lin, and J.J. Zhong, "3D vector magnetic properties of soft magnetic composite material," *Journal of magnetism and magnetic materials*, vol. 302, no. 2, pp. 511-516, 2006.

[6] N. Nencib, A. Kedous-Lebouc, and B. Cornut, "2D analysis of rotational loss tester," *IEEE Transactions on Magnetics*, vol. 31, no. 6, pp. 3388-3390, 1995.

[7] C. Ragusa and F. Fiorillo, "A three-phase single sheet tester with digital control of flux loci based on the contraction mapping principle," *Journal of Magnetism and Magnetic Materials*, vol. 304, no. 2, pp. e568-e570, 2006.

[8] C. Appino, F. Fiorillo, and C. Ragusa, "One-dimensional/two-dimensional loss measurements up to high inductions," *Journal of Applied Physics*, vol. 105, no. 7, p. 07E718, 2009.

[9] G. Bertotti, "General properties of power losses in soft ferromagnetic materials," *IEEE Transactions on Magnetics*, vol. 24, no. 1, pp. 621-630, 1988.

[10] Höganäs SMC Brochures. [Online]. http://www.hoganas.com/en/Products--Applications/Soft-Magnetic-Composites/SMC-Brochures-Pics/

[11] M. Enokizono and J.D. Sievertt, "Magnetic field and loss analysis in an apparatus for the determination of rotational loss," *Physica Scripta*, vol. 39, pp. 356-359, 1989.

[12] O. de la Barrière et al., "Loss separation in soft magnetic composites," *Journal of Applied Physics*, vol. 109, p. 07A317, 2011.

[13] C. Ragusa, C. Appino, and F. Fiorillo, "Magnetic losses under two-dimensional flux loci in Fe–Si laminations," *Journal of magnetism and magnetic materials*, vol. 316, no. 2, pp. 454-457, 2007.

Figure captions

Fig. 1: Experimental equipment. The disk-shaped SMC sample is put in the center of the three phase stator.

Fig. 2: Total energy loss per cycle under alternating sinusoidal induction and circular induction as a function of the frequency f, for different B_P values.

Fig. 3: Hysteresis loss ratio $R_{hyst}(B_P)=W_{hyst}^{(circ)}(B_P)/W_{hyst}^{(alt)}(B_P)$ versus the peak induction B_P

Fig. 4: Excess loss ratio $R_{exc}(B_P)=W_{exc}^{(circ)}(B_P,f)/W_{exc}^{(alt)}(B_P,f)$ versus the peak induction B_P, for different frequencies f (from 0 to 4 kHz)

Fig. 5: Measurement and prediction of the loss under elliptical induction loci for two different frequencies f=100 Hz and 1000 Hz (the major axis has an amplitude kept constant equal to B_P=1 T, and the minor axis amplitude B_M undergoes a variation trough the parameter $a=B_m/B_P$). The open circles are the experimental loss W, compared to the prediction (continuous line). The dotted line corresponds to the computed hysteresis component $W_{hyst}^{(ellip)}$, while the dashed line represents the sum $W_{hyst}^{(ellip)}+W_{class}^{(ellip)}$.

136 **Figures**

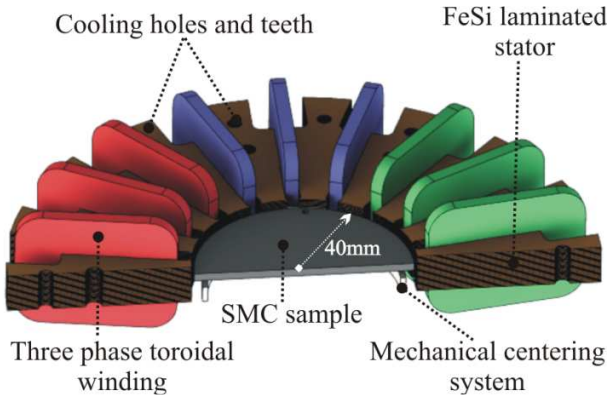

137
138 Fig. 1

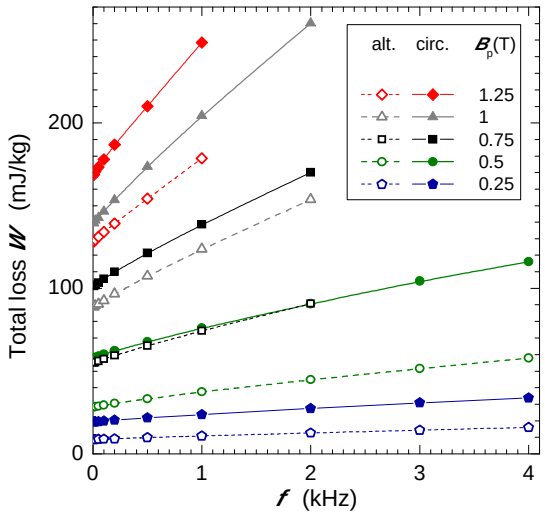
alt.
circ.
B_p(T)
1.25
1
0.75
0.5
0.25
Total loss W (mJ/kg)
200
100
0
0
1
2
3
4
f (kHz)

Fig. 2

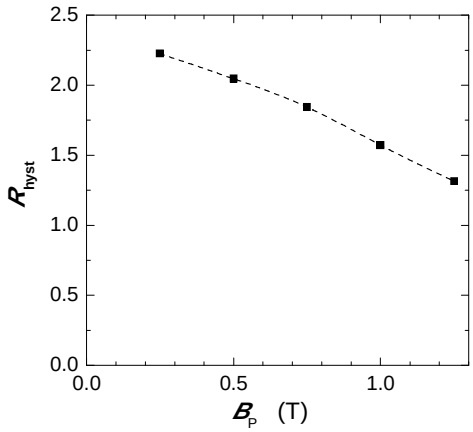

141

142 Fig. 3

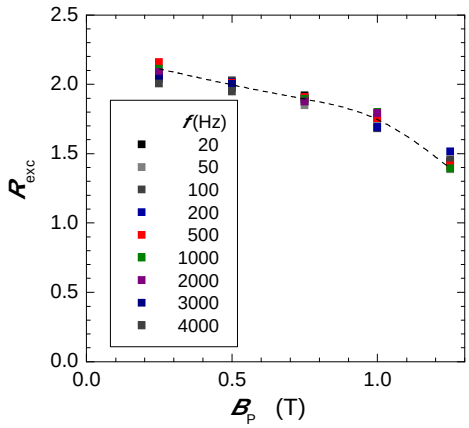
2.5
2.0
1.5
1.0
0.5
0.0
0.0
0.5
1.0
R_{exc}
B_p (T)
f(Hz)
20
50
100
200
500
1000
2000
3000
4000

143

144 Fig. 4

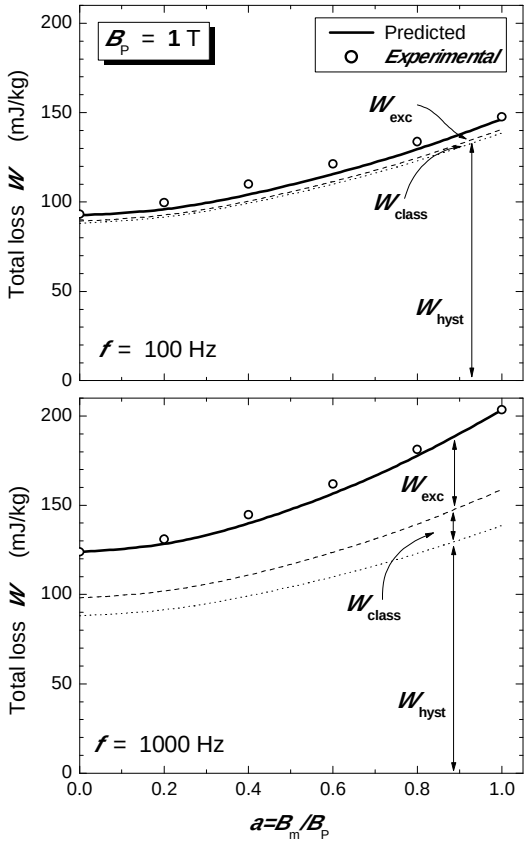
B_P = 1 T
Predicted
Experimental
W_{exc}
W_{class}
W_{hyst}
f = 100 Hz
Total loss W (mJ/kg)
f = 1000 Hz
$a=B_m/B_P$

Fig. 5